Study on the Influence of Aerodynamic Effect of High-speed Maglev Train Crossing Underground Tunnel Station

Yinxiao Liao[1, a]

[1]Qingdao University of Technology, Qingdao, China

[a]2104711788@qq.com

Abstract. The maximum speed of rail trains with a traditional wheel-rail contact relationship is limited. Under this background, high-speed maglev transportation with a higher speed level becomes a possible solution. With the increase in the operating speed of maglev trains, a series of aerodynamic problems have arisen, especially when the train passes through the underground tunnel station in the city, where the pressure wave problem is more prominent than on the open line. Therefore, it is necessary to study the formation mechanism of the pressure wave and the influence of aerodynamic effects when the high-speed maglev train passes through the tunnel station. In this paper, a three-dimensional finite element model of a high-speed maglev train-tunnel station is established, and the aerodynamic effect of a high-speed maglev train passing through the tunnel platform is studied and analyzed using the k−ε turbulence model. The main conclusions are as follows: the peak pressure of the train will increase with the increase of train speed, and the amplitude of its pressure wave head is related to the 2~3 power of train speed; Setting a vertical shaft next to the underground tunnel station will reduce the pressure on trains and stations to some extent, and the average pressure reduction rate can reach about 43%. Therefore, it is of great engineering significance to carry out this research on the construction of underground maglev train stations and to ensure the safe passage of high-speed maglev trains through underground stations.

Keywords: Vertical shaft, high-speed maglev train, aerodynamic effect, pressure wave.

1. Introduction

As a new type of rail transit in the 21st century, the high-speed maglev train runs at a maximum speed of 400~600 km/h under normal pressure, which can fill the speed fault between high-speed railway (350 km /h) and air transportation (800~1000 km /h), increase the choice of transportation modes at different speed segments, and further improve the modern comprehensive transportation system [1]. Compared with the traditional wheel-rail transportation system, maglev train has the advantages of small friction resistance, strong climbing ability, fast running speed, safety and punctuality, energy saving and environmental protection, comfort, and high efficiency [2]. So far, many countries worldwide have done a lot of research on maglev trains and have achieved remarkable results. The L0 maglev train, independently developed by Japan in 2015, set a world record of 603 km/h for maglev manned trains [3]. On June 21, 2020, the 600km/h high-speed maglev test vehicle in China was successfully tested on the maglev test line established by Tongji University in Shanghai [4], which marked a major breakthrough in the research of high-speed maglev trains in China. However, when the train passes through the city, there will be a series of problems, such as occupying urban land, reducing urban green area, and affecting residents' normal life. Therefore, in future construction, it may be considered to put high-speed maglev trains under the city and set up underground stations. However, the aerodynamic effect of the train running in the tunnel will be far different from that of the open line. For example, when the train passes the station, pressure and train wind act on the roadside personnel and surrounding objects, which may endanger the life safety of passengers and operators on the platform, and even cause the platform screen door to burst or the objects on the platform to be rolled up, endangering the safety of train operation [5].

In recent years, relevant scholars have continuously studied the aerodynamic effects of medium and low-speed maglev trains passing through tunnels. For example, the influence of train body length on aerodynamic effect. Analysis of aerodynamic effect of medium and low speed maglev train: Guidance of cryogenic superconducting maglev train, etc. YAMAMOTO found that the amplitude of micro-pressure is proportional to the pressure gradient of the compression wave at the tunnel exit [6]. HOWE investigated the variation curve of compression wave in a tunnel and put forward the calculation formula of maximum pressure gradient [7]. Sun Z et al. used a multi-objective genetic algorithm and a complex three-dimensional geometric parameterization method to optimize the streamlined head of the train. They obtained several optimal shapes [8]. A sliding mode control (SMC) method proposed by Liu et al. can effectively suppress the electromagnetic fluctuation of trains under pneumatic load [9]. Che Z et al. proposed an effective active flow control method to reduce the aerodynamic drag of trains [10].

In earlier years, a large number of scholars studied the aerodynamic effects of traditional wheel-rail trains passing through station tunnels. Han Huaxuan took the Meilan International Airport underground station tunnel as the research background. He used numerical simulation and model test to explore the aerodynamic environment, such as pressure fluctuation, transient pressure, and wind speed in the station under different underground station tunnel design parameters [11]. Xie Hongtai used the finite volume numerical simulation method to analyze and calculate high-speed trains running in extra-long double-track tunnels' local flow field structure and pressure wave distribution [12]. Zhao J et al. established a flow geometric model according to the actual situation of the flow field when the train passed through the tunnel, and mainly analyzed the pressure change in the tunnel caused by the high-speed train entering the tunnel and the mechanical characteristics of the carriage when two trains passed through each other in the tunnel [13]. Friedl et al. took a new high-speed train track in Austria as the research background, measured the aerodynamic effects of different train types, and discussed the correlation between the aerodynamic effects of the sound barrier wall and the dynamic wave characteristics [14].

The above contents mainly focus on the research of maglev trains passing through the tunnel and the aerodynamic effect of traditional wheel-rail trains passing through the tunnel and platform, but there is a lack of research on high-speed maglev trains passing through the station in the tunnel. When the train enters the tunnel and passes through the station at high speed, due to the airspace, the transient changes of pressure and speed will be aggravated [15], and the boundary of the flow field around the train will suddenly change, resulting in an unstable flow field with dynamic pressure and velocity. These pressure and velocity transients will cause harm to people, objects, and buildings beside the track [16]. However, in this narrow confined space, the main aerodynamic effect caused by the train in the tunnel is the change of pneumatic pressure. The train head enters the tunnel, resulting in a compressional wave. The tail car enters the tunnel and produces an expansion wave. They propagate, reflect, and overlap in the tunnel, resulting in huge transient pressure. These problems need to be studied urgently when applied to tunnel walls, train surfaces, and station screen doors [17-20].

In this paper, the aerodynamic effects and pressure waves generated by the 600km/h high-speed maglev train passing through the station in the tunnel are studied, and a series of studies are made on the aerodynamic effects of the high-speed maglev train passing through the station scene by using the k−ε turbulence model. This study provides a theoretical basis for the design and construction of the high-speed maglev train station and is of great significance for ensuring the high-speed maglev train passes through the station safely.

2. Calculation Model

2.1. Geometric Model

2.1.1. Train model

The train model is a full-scale high-speed maglev train, consisting of five groups: the head, three intermediate cars, and the tail car. The three-dimensional model of the train is shown in Figure 2.1. The train head is 3.06m high, 3.68m long, and 132.71m long.

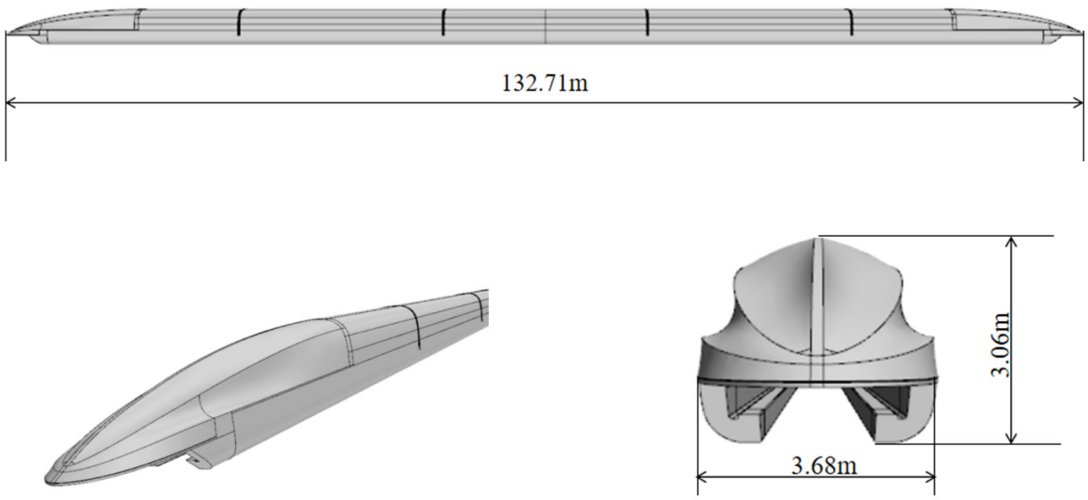

Figure 2.1 Maglev Train Model

2.1.2. Station model

The geometric model of an underground maglev train station is shown in Figure 2.2. The station yard is divided into the line, equipment, and platform waiting areas. In this paper, a double-island-sandwiched four-line station is adopted, that is, four maglev track lines are sandwiched between platforms on both sides, two of which are crossing lines in the middle and two of which are arrival and departure lines near the platform. Screen doors are set on both sides, and the equipment area is located in the four corners of the station platform. Only one corner is shown in the figure.

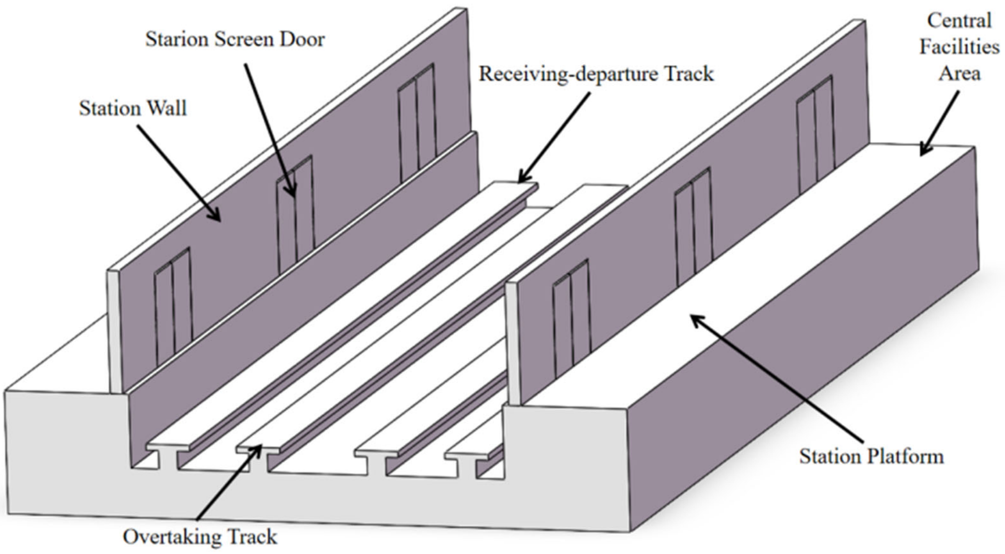

Figure 2.2 Station Model

2.1.3. Vertical shaft model

The numerical calculation model of the vertical shaft position is shown in Figure 2.3. The length of the train station is set to D = 275m. The vertical shaft is set at a distance of 0m from both ends of the station, with a height of H = 30m and an opening ventilation area of S = 25m^2.

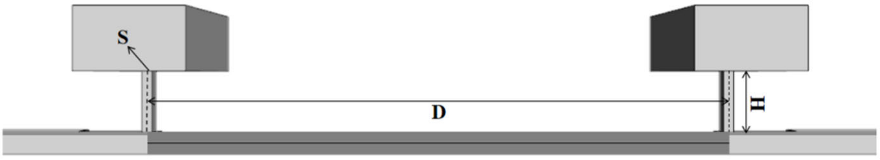

Figure 2.3 Parameter Design of vertical Shaft Model

2.2. Grid Model

This study uses the STAR-CMM+ simulation software to mesh the underground maglev train and its surrounding air domain. The grid division of the maglev train is shown in Figure 2.4. The basic size of the train body surface grid is set to 0.05m, and the minimum grid size is 0.025m. Because the train is in the core area of motion, the boundary layer greatly influences the air flow, so a separate surface grid control is set on the train surface. The basic size of the surface of this additional layer is 0.01m, and the minimum grid size is 0.0005m. When the speed of the maglev train is 600km/h, the value of y+ is about 40, which ensures that the wall function of y+ is within a reasonable range. The volume grid near the car body is set as an encryption area with a size of 0.1m. Overlapping grids are used around the train body, the grid size is set to 0.2m, and the number of grids is about 17 million.

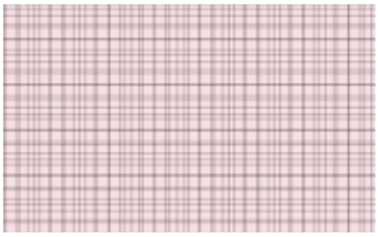

(A) The Peripheral Surface of the Vehicle body

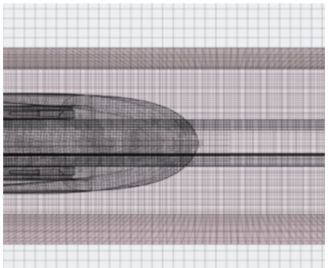

(B) Track Surface

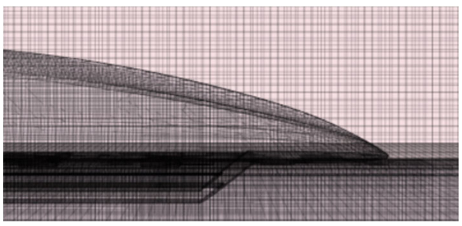

(C) Body Surface

Figure 2.4 Grid distribution around maglev train

2.3. Layout of Measuring Points

To study the aerodynamic load on the screen door when the high-speed maglev train passes through the underground station, the corresponding wind pressure monitoring points are arranged on the surface of the screen door of the arrival-departure station. To study the distribution law of wind pressure along the longitudinal direction, this paper gives a schematic diagram of the distribution of measuring points along the longitudinal direction, as shown in Figure 2.5. The arrival and departure lines are evenly distributed along the train's running direction. The X coordinates corresponding to the longitudinal measuring points are 12.5m, 37.5m, 62.5m, 87.5m, 112.5m, 137.5m, 162.5m, 187.5m, 212.5m, 237.5m and 262.5m respectively, and the interval between every two adjacent measuring points is 25m, and the height is 1.5m.

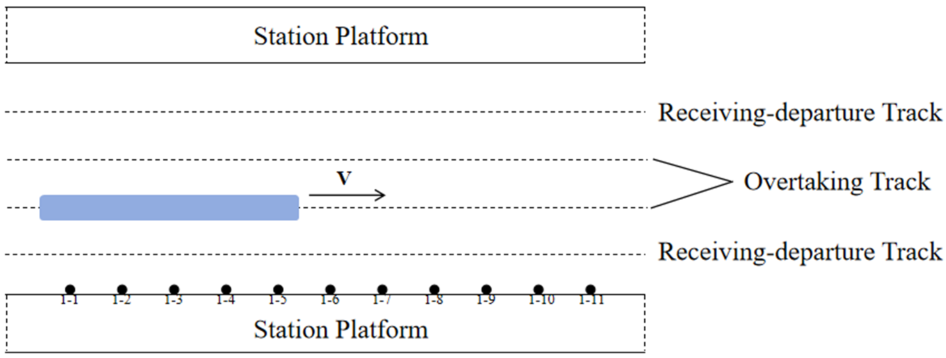

Figure 2.5 Schematic Diagram of Longitudinal Distribution of Measuring Points

To study the influence of vertical height on aerodynamic load when the high-speed maglev train crosses the station at a speed of 600km/h, corresponding measuring points are arranged on the surface of the arrival and departure line screen door, and the vertical distribution of measuring points is shown in Figure 1.8. The vertical measuring points are distributed on three interfaces: station entrance x=37.5m, station center x = 137.5m, and station exit x = 237.5 m. Vertical measuring points are evenly arranged from 0m to 3m along the height direction, and the interval between every two adjacent measuring points is 0.5m.

3. Dynamic Model Verification

In order to verify the correctness of the numerical simulation method used in this paper, the numerical simulation results are analyzed and compared with the dynamic model test results. In the dynamic model test, a 3-car high-speed maglev train was used, with a tunnel length of 320 m and a clearance area of 100 m^2, and the model scale was 1:20 [21]. Figure 3.1 and Table 3.1 show that the numerical simulation calculation adopted in this paper is in good agreement with the dynamic model test results. The relative error of the positive peak value and the negative peak value of the tunnel wall pressure is 0.041% and 2.243%, and the error range is within 5%, which verifies the accuracy of the calculation model and numerical calculation in this paper.

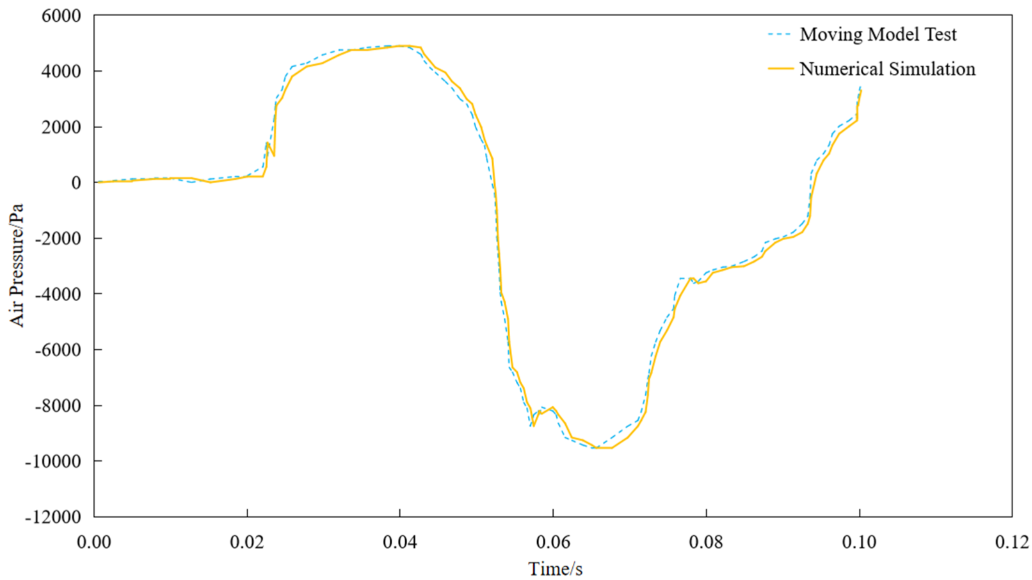

Figure 3.1 Time-history Curve of Tunnel Wall Pressure Measuring Points

Table 3.1 Results of Comparison of Numerical Simulation and Dynamic Model Test

Type	Tunnel Wall Pressure/Pa	
	Positive Peak	Negative Peak
Moving Model Test	4899.9	-9531.01
Numerical Simulation	4901.9	-9300.1
Relative Error	0.041%	2.423%

4. The Pressure Wave Analysis of Influencing Factors

4.1. Pressure Wave Propagation Characteristics

When the train enters the tunnel at high speed, the air at the tunnel entrance is compressed sharply at the moment the train head enters, and the space around the train head is reduced, thus compressing the wave in the first section at the train head. At this time, the compression wave propagates along the tunnel axis at the speed of sound and squeezes the air in front of the tunnel. At this time, the pressure will rise rapidly, and the pressure at the head of the train will also rise.

When the rear of the train enters the tunnel, the air that starts to flow out of the tunnel entrance through the annular space cannot flow out smoothly, but only flows into the tunnel behind the train, where it is violently turbulent and mixed with the air in the tunnel. The pressure drops relative to the atmospheric pressure at the entrance, so the first expansion wave is generated and propagates along the annular space, accelerating the backward flow of the annular air flow, as shown in Figure 4.1.

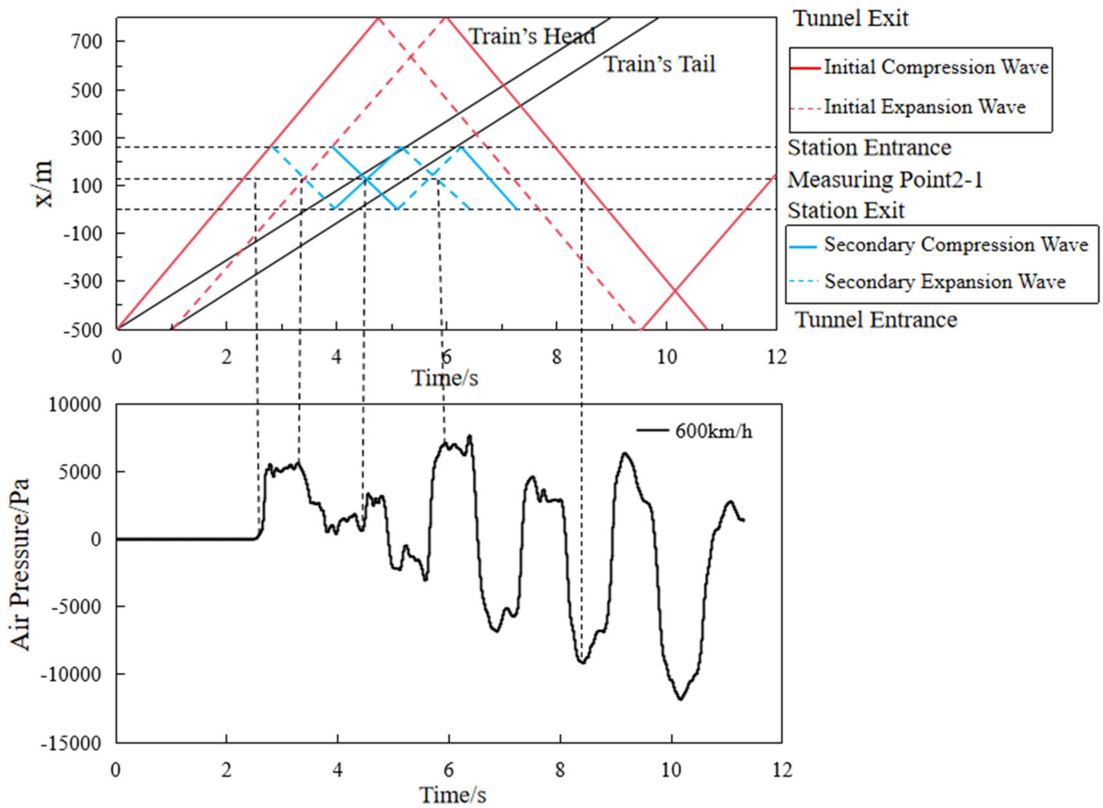

Figure 4.1 Pressure Wave Propagation Process Diagram of Underground Maglev Station

4.2. Pressure Wave Distribution Law

Figure 4.2 shows the peak pressure variation curve of 11 longitudinal measuring points (Figure 1.7) when the high-speed maglev train passes through the station screen door at a speed of 600km/h and there are no vertical shafts on both sides of the station. As can be seen from Figure 2.2, on the same horizontal line, the peak pressure of measuring point 1-6 is the largest (x=137.5m), so the velocity simulation analysis is made for measuring point 1-6.

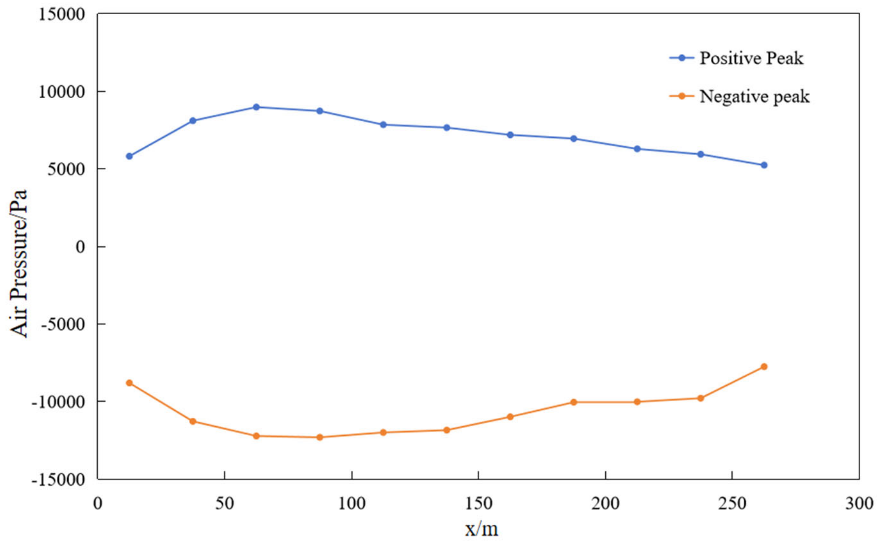

Figure 4.2 The Diagram of Pressure Peak Changing with Position

4.3. The Influence of Speed

According to the analysis of the numerical simulation results mentioned above, it can be concluded that the pressure change of the train in the middle section of the screen door is the most obvious, and the amplitude is the largest. Therefore, measuring points 1-6 are selected to carry out numerical simulation tests when the train crosses the screen door at 400km/h, 500km/h, and 600km/h, respectively, and Figure 4.3 is obtained.

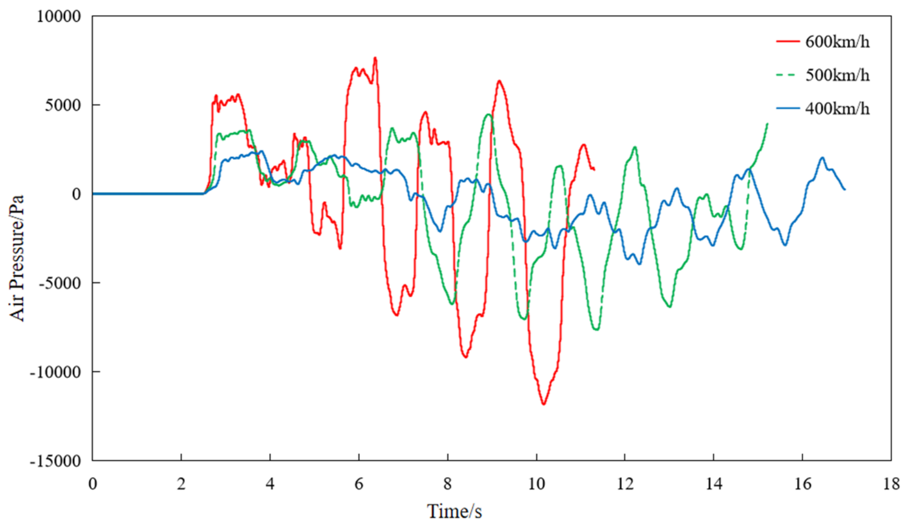

Figure 4.3 Pressure Change Diagram at Different Speeds

As can be seen from the figure, when the underground high-speed maglev train crosses the station screen door, the change of train speed greatly influences the pressure on the surface of the screen door. Because the pressure of the station screen door will increase with the train crossing speed, the first peak value of the pressure wave will increase with the increase of the crossing speed, and the peak value will appear earlier. And the maximum pressure of each positive and negative peak gradually increases, and the maximum peak pressure difference is also increasing. After the first pressure wave, the occurrence time of the pressure peak began to advance.

The pressure wave of an underground high-speed maglev train greatly correlates with the crossing speed, as shown in Figure 4.4. As can be seen from the figure, the first pressure wave will increase with the increase in velocity. At 500km/h, the first wave amplitude at the entrance, central station and exit section is 78.68%, 86.11% and 91.87% higher than that at 400km/h, and at 600km/h, the first wave amplitude is 206.43%, 219.52% and 239.01 higher than that at 400km/h, respectively. The relationship between the amplitude and speed of the first wave is fitted, and the relationship between the amplitude of the first wave and the crossing speed is 2~3 power.

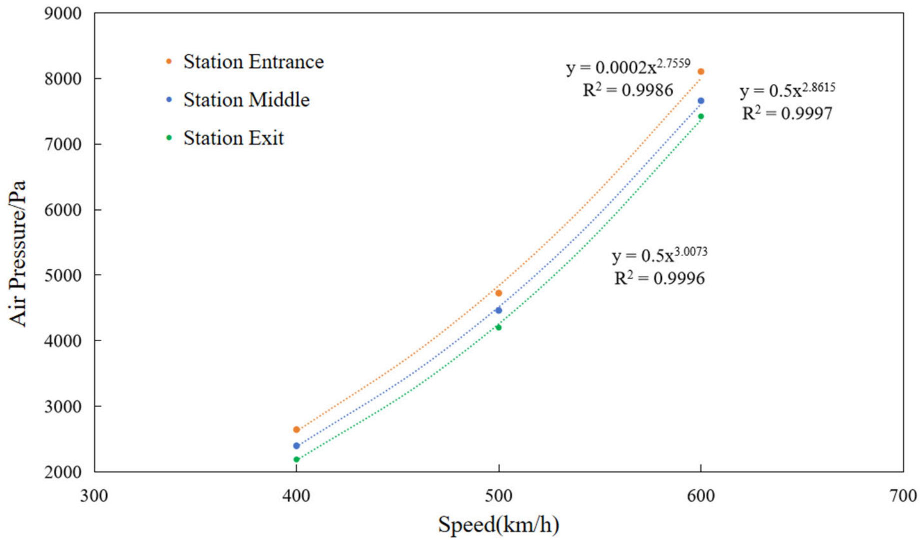

Figure 4.4 Relationship Between Pressure Wave Head Amplitude and Crossing Speed

4.4. Influence of Shaft on Aerodynamic Effect of High-speed Maglev Train Passing Station

4.4.1. Analysis of the principle of vertical shaft pressure relief

When the high-speed maglev train enters the tunnel, it is no different from the tunnel without a shaft. When the train head enters the tunnel, it will generate compression waves. When the train completely enters the tunnel, the analysis of the air flow field in the tunnel can be divided into three stages, namely, before the train reaches the shaft, when the train reaches the shaft position, and when the train tail reaches the shaft position, as shown in Figure 4.5.

The first stage is that after the train enters the tunnel, it produces the first compression wave and reaches the position of the vertical shaft. This compression wave will propagate upward in the form of compression wave 1 and forward in the form of compression wave 2, and this process will lose part of the energy of this compression wave. When the compression wave 1 reaches the top of the shaft, part of it propagates to the outside atmosphere, losing most of the energy, and the rest propagates to the bottom of the shaft in the form of an expansion wave. When the expansion wave reaches the tunnel, it is divided into expansion wave 2 and expansion wave 3, which propagate to the front and back of the tunnel, respectively. When these waves reach the tunnel mouth, part of them will propagate back in this form, and so on until the energy of the waves is exhausted.

The second stage is to generate a compression wave 3 when the train reaches the shaft position. This compression wave will be divided into compression wave 4 and compression wave 5, which will propagate in a form similar to the first compression wave. Part of the compression wave 5 propagates to the outside atmosphere, and part of it is reflected back in the form of expansion wave 3, which is divided into expansion wave 4 and expansion wave 5 and propagates to the front and back of the tunnel. Repeating this until the energy of the wave is exhausted.

In the third stage, when the train tail passes through the shaft position, expansion waves 6 and 7 will be generated at the train tail. The expansion wave 6 propagates upward, in a propagation form similar to that of the first compression wave, and generates a compression wave 6 that propagates downward. After reaching the tunnel, the compression wave 6 propagates back and forth in the form of compression wave 7 and compression wave 8. In this way, the energy of the wave is exhausted in the form of the first stage.

In the whole stage, when the compression wave and expansion wave are divided into two propagation forms, some energy will be consumed, thus achieving the effect of pressure relief.

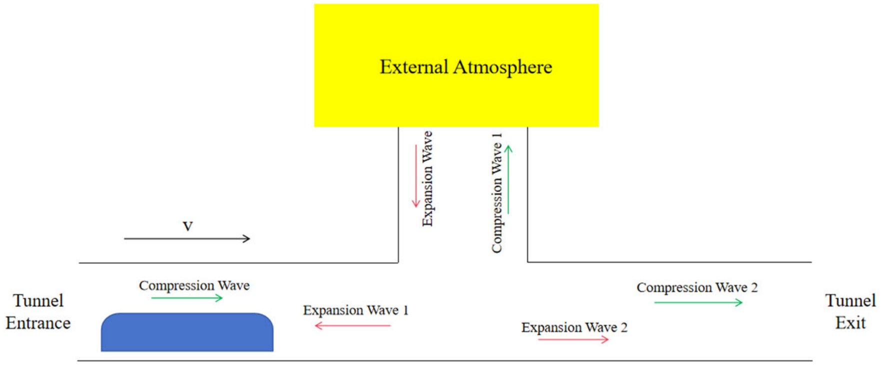

(A) Phase I

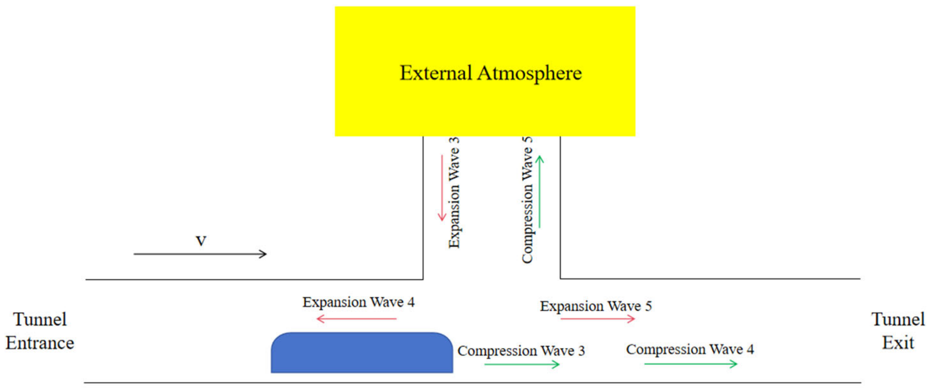

(B) Phase II

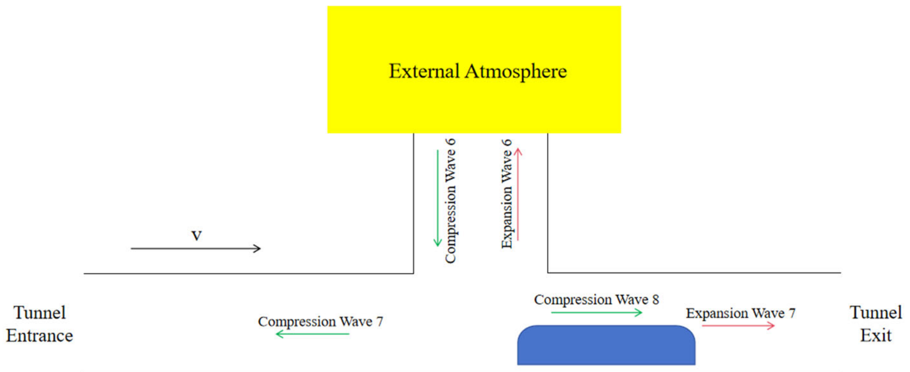

(C) Phase III

Figure 4.5 Influence of Vertical Shaft on Pressure Propagation

4.4.2. Influence of Vertical Shaft on Pressure Wave

Figure 4.6 shows the influence of the shaft on the surface wind pressure of the screen door. It can be seen that the influence of the shaft on the pressure changes most significantly at measuring point 1-11, with the maximum pressure peak reduced by 50.25% and the average pressure peak reduced by more than 40%. The average peak pressure of the three measuring points 1-2, 1-8, and 1-11 decreased by more than 30%.

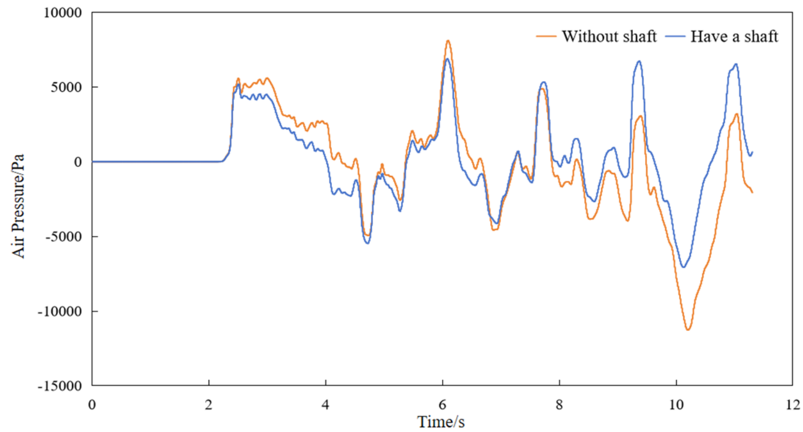

(A) Diagram of Pressure Changing with Time at Measuring Point 1-2.

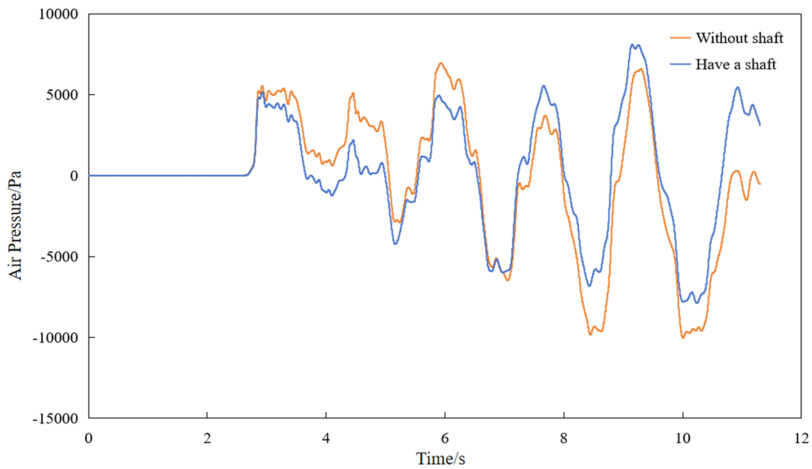

(B) Diagram of Pressure Changing with Time at Measuring Point 1-8.

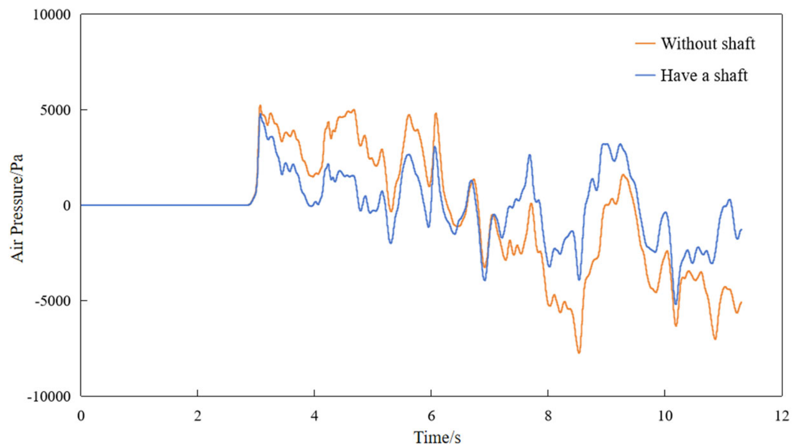

(C) Diagram of Pressure Changing with Time at Measuring Point 1-11.

Figure. 4.6 Pressure variation with time at different measuring points.

Figure 4.7 compares the positive and negative pressure peaks with or without a vertical shaft. It can be seen that the positive pressure peaks at x=37.5m and 62.5m have the best pressure relief effect, and the pressure peaks are reduced by 15.04% and 15.60% respectively. The negative pressure peaks at x=37.5m and 237.5m have the best pressure relief effect, and the pressure peaks are reduced by 37.29% and 35.42% respectively. Among them, the positive value in the table 4.1 represents the pressure relief effect, and the negative value means the pressurization effect.

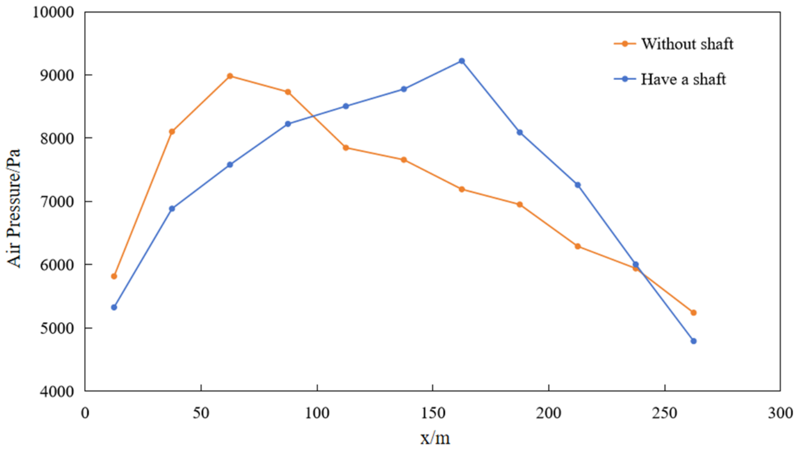

(A) Diagram of Positive Peak Pressure Changing with Coordinates

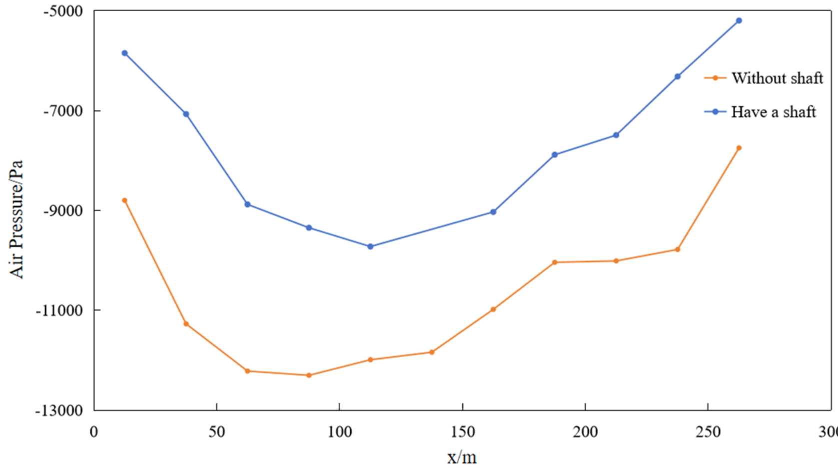

(B) Diagram of Negative Peak Pressure Changing with Coordinates

Figure 4.7 Diagram of Pressure Peak with or Without Vertical Shaft Changing with Coordinates

Table 4.1 Pressure Peak Reduction Rate at Different Positions

Longitudinal position x(m)	Positive pressure peak	Negative pressure peak
12.5	8.44%	33.54%
37.5	15.04%	37.29%
62.5	15.60%	27.32%
87.5	5.79%	24.02%
112.5	-8.37%	18.91%
137.5	-14.58%	19.66%
162.5	-28.21%	17.77%
187.5	-16.40%	21.47%
212.5	-15.44%	25.17%
237.5	-1.06%	35.42%
262.5	8.57%	32.93%

5. Conclusions

In this paper, the finite element model of the underground high-speed maglev train-station flow field is established, and the influence law of aerodynamic effect when the underground high-speed maglev train passes through the underground station at a speed of 600km/h is analyzed. The influence of setting vertical shafts on the pressure wave mitigation effect is studied, and the following main conclusions are drawn:

(1) When the underground high-speed maglev train crosses the station, the peak pressure of the train will increase with the increase of the train speed, and the amplitude of the pressure wave head is related to the 2~3 power of the train speed. When the train speed increases from 400km/h to 500km/h, the peak value of pressure wave increases by 47.78%-92.26%; When the train speed is increased from 400km/h to 600km/h, the peak value of pressure wave increases by 119.84%-241.91%. Therefore, when the high-speed maglev train passes the station at a speed of 600km/h, the peak pressure wave will rise significantly.

(2) Setting vertical shafts on both sides of underground tunnel stations will reduce the pressure of trains and stations to some extent, and vertical shafts can reduce the average peak pressure of station screen doors by about 43%, thus reducing the harm to trains and stations to some extent.

(3) In this paper, the strong aerodynamic effect that may occur when the underground high-speed maglev train crosses the underground station is modeled and analyzed, and the influence of setting up shafts on both sides of the underground station on the reduction of peak pressure is studied, which provides a theoretical basis for ensuring the train to pass through the station safely and provides some support for future engineering construction. However, there are still many shortcomings and improvements in this study, so in future research, we can also analyze, design, and optimize the surface pressure of the train, the structure of the station building and its ancillary equipment, and the structural parameters of the vertical shaft.

References

[1] Yu Haowei, Kou Junyu, Li Yan. Adaptability and engineering development of 600 km/h high-speed maglev in China [J]. Journal of Railway Engineering Society, 2020,37(12):16-20+88.

[2] Ren Kuishan. Preliminary study on aerodynamic effect of the buffer structure at the entrance of a 600km/h maglev railway tunnel [D]. Lanzhou Jiaotong University, 2021. DOI: 10.27205/d.cnki.gltec.2021.200800000003

[3] Zhang Jie, Wang Yuge, Han Shuai, et al. Analysis of the influence of buffer structure length on the pressure wave characteristics of a 600 km/h maglev train passing through the tunnel [J]. Journal of Central South University (Natural Science Edition), 2022,53(05):1668-1678.

[4] Yu Haowei, Kou Junyu, Li Yan. Adaptability and engineering development of 600 km/h high-speed maglev in China [J]. Journal of Railway Engineering Society, 2020,37(12):16-20+88.

[5] Tan Haiou, Feng Haiquan, WangZhifei, et al. Study on the influence of high-speed trains passing through the station on the surface air pressure load of the platform screen door [J]. Modern urban rail transit, 2022,(11):30-35.

[6] YAMAMOTO A. Aerodynamics of train in tunnel[C]// Japan: Proc Lecture Meeting of the RTRI, 1975: 13−16.

[7] HOWE M S. On the compression wave generated when a high-speed train enters a tunnel with a flared portal[J]. Journal of Fluids and Structures, 1999, 13(4): 481−498.

[8] Sun Z, Wang M Y, Wei L Y, et al. Aerodynamic shape optimization of an urban maglev train[J]. 2021.DOI:10.1007/s10409-021-01094-y.

[9] Liu M, Wu H, Xu J, et al. Research on sliding mode controller of the high-speed maglev train under aerodynamic load[J]. Advances in Mechanical Engineering (Sage Publications Inc.), 2022. DOI:10.1177/16878132221127857.

[10] Che Z, Huang S, Li Z, et al. Aerodynamic drag reduction of high-speed maglev train based on air blowing/suction[J]. Journal of Wind Engineering and Industrial Aerodynamics, 2023.DOI:10.1016/j.jweia.2023.105321.

[11] Han Huaxuan. Study on Aerodynamic Effects and Mitigation Measures of High-speed Railway Underground Station Tunnel [D]. Southwest Jiaotong University, 2010.

[12] Xie Hongtai. Numerical simulation analysis of surface pressure distribution of 350 km/h high-speed train passing through extra-long double-track tunnel [J]. Journal of East China Jiaotong University, 2019,36 (04): 24-31. doi: 10.16749/j.cnki.jecjtu.2019.04.004.

[13] Zhao J, Li R. A STUDY OF AERODYNAMIC EFFECTS OF HIGH-SPEED TRAINS THROUGH TUNNELS[C]//International Conference on Civil Engineering and Transportation 2011.

[14] Friedl H, Reiterer M, Kari H. Analysis of Aerodynamic Impact induced by High Speed Trains[C]//The Fourteenth International Conference on Civil, Structural and Environmental Engineering. 2013.DOI:10.4203/ccp.102.26.

[15] Liang X F, Chen G, Li X B, et al. Numerical simulation of pressure transients caused by high-speed train passage through a railway station[J]. Building and Environment, 2020:107228. DOI: 10.1016/j.buildenv.2020.107228.

[16] Zhou D, Tian H Q, Zhang J, et al. Pressure transients induced by a high-speed train passing through a station - ScienceDirect[J]. Journal of Wind Engineering and Industrial Aerodynamics, 2014, 135:1-9. DOI:10.1016/j.jweia.2014.09.006.

[17] Kim J Y, Kim K Y. Experimental and numerical analyses of train-induced unsteady tunnel flow in subway[J]. Tunnelling & Underground Space Technology Incorporating Trenchless Technology Research, 2007, 22(2):166-172. DOI: 10.1016/j.tust.2006.06.001.

[18] Liu T H, Chen X D, Li W H, et al. Field study on the interior pressure variations in high-speed trains passing through tunnels of different lengths[J]. Journal of Wind Engineering and Industrial Aerodynamics,2017, 169:54-66. DOI: 10.1016/j.jweia.2017.07.004.

[19] Zhang H, Zhu C, Liu M, et al. Mathematical modeling and sensitive analysis of the train-induced unsteady airflow in subway tunnel[J]. Journal of Wind Engineering and Industrial Aerodynamics, 2017, 171:67-78. DOI: 10.1016/j.jweia.2017.09.005.

[20] Liu T, Jiang Z, Chen X, et al. Wave effects in a realistic tunnel induced by the passage of high-speed trains [J]. Tunnelling & Underground Space Technology, 2019, 86(APR.): 224-235. DOI:10.1016/j.tust.2019.01.023.

[21] Zhang Jie, Wang Yuge, Han Shuai, et al. Analysis of the influence of buffer structure length on the pressure wave characteristics of a 600 km/h maglev train passing through the tunnel [J]. Journal of Central South University (Natural Science Edition), 2022,53(05):1668-1678.